has shown that the compounds 8 eliminate H_2 and add CO under mild conditions.

Although 2 can be converted into 3 at 125 °C, it was observed that significant amounts of 3 were also formed in the original preparation of 2 (98 °C). We have not been able to transform 2 to 3 at these milder conditions. Thus, we have considered the possibility of a route from 1 to 3 that does not involve a CO dissociative step (Scheme V). Cleavage of the Os–N bond in 1 would yield a terminally coordinated (dimethylamino)methyl ligand with a vacant site on the neighboring metal atom, F. C–H activation of the methylene group would yield intermediate G containing a C-coordinated bridging carbene ligand and ten carbonyl ligands. However, except for those complexes that contain dihapto triply bridging aminocarbene ligands,[9] in all examples of cluster complexes containing (dialkylamino)carbene ligands, the carbene ligands are found to adopt terminal bonding modes.[4,5,7-9] This may be due to the strong tendency of the lone pair of electrons on the nitrogen atom to donate to the carbene carbon atom and thus prevent the formation of the second metal–carbon bond. Accordingly, it seems likely that the intermediate G would convert to an isomer like H having a terminally coordinated carbene ligand. Loss of H_2 from H could generate a vacant site on the metal atom adjacent to the carbene ligand, I, and a subsequent α-CH activation of the carbene C–H bond would lead directly to the product 3. Binuclear α-CH activations in secondary (dialkylamino)-carbene ligands have been observed previously.[8]

Several years ago, Deeming reported that compound 3 was obtained in a low yield from the reaction of $Os_3(CO)_{12}$ and NMe_3 at high temperature.[13] The compounds 1 and 2 that were prepared under the much milder conditions reported here now appear to provide the first evidence of a rational pathway for this reaction.

The transformation behavior of the (dimethylamino)-methyl ligand in this series of triosmium cluster complexes shows similarities to the transformation of the methyl group in the $Os_3(CO)_{10}(\mu\text{-}CH_3)(\mu\text{-}H)$, $Os_3(CO)_{10}(\mu\text{-}CH_2)(\mu\text{-}H)_2$, and $Os_3(CO)_9(\mu_3\text{-}CH)(\mu\text{-}H)_3$ series studied by Shapley.[21] The C–H activation processes are based upon multicenter interactions of the ligand with the triosmium group. It is expected that these processes will be general in nature. Similar transformations have been observed for bridging thioformaldehyde ligands in triosmium clusters.[22] The ability of cluster complexes to produce novel ligand transformations and catalysis is proving to be an intrinsic feature of their chemistry.

Acknowledgment. These studies were supported by the Office of Basic Energy Sciences of the U.S. Department of Energy. We wish to thank Johnson-Matthey Inc. for a loan of osmium tetraoxide. The Brüker AM-300 NMR spectrometer was purchased with funds from the National Science Foundation under Grant No. CHE-8411172.

Registry No. 1, 112839-61-9; 2, 112839-62-0; 3, 63373-87-5; $Os_3(CO)_{10}(\mu\text{-}H)_2$, 41766-80-7; $CH_2(NMe_2)_2$, 51-80-9.

Supplementary Material Available: Tables of positional parameters and anisotropic thermal parameters for compounds 1, 2, and 3 (9 pages); listings of structure factor amplitudes for compounds 1, 2, and 3 (40 pages). Ordering information is given on any current masthead page.

(21) Keister, J. B.; Payne, M. W.; Muscatella, M. J. *Organometallics* **1986**, *2*, 219.
(22) Calvert, R. B.; Shapley, J. R. *J. Am. Chem. Soc.* **1977**, *99*, 5226.
(23) Adams, R. D.; Babin, J. E.; Tasi, M. *Organometallics* **1987**, *6*, 1717.

Polynuclear Acetylides. Synthesis, Spectroscopic Features, and Structural Systematics for a Complete Triad of μ_2-η^2-Complexes: $M_2(CO)_6(\mu_2\text{-}\eta^2\text{-}C{\equiv}CR)(\mu\text{-}PPh_2)$ (M = Fe, Ru, Os)

Andrew A. Cherkas, Leslie H. Randall, Shane A. MacLaughlin, Graham N. Mott, Nicholas J. Taylor, and Arthur J. Carty*

Guelph-Waterloo Centre for Graduate Work in Chemistry, Department of Chemistry, University of Waterloo, Waterloo, Ontario, Canada N2L 3G1

Received September 25, 1987

The synthesis of the triad of phosphido-bridged, acetylide-bridged dimetallic carbonyls $M_2(CO)_6(\mu_2\text{-}\eta^2\text{-}C_2R)(\mu\text{-}PPh_2)$ (1, M = Fe; 2, M = Ru; 3, M = Os; a, R = Ph, b, R = *t*-Bu, c, R = *i*-Pr) is described. The molecules 1, 2, and 3 were prepared via pyrolysis of $M_3(CO)_{11}(Ph_2PC{\equiv}CR)$ which initiates metal metal bond cleavage and oxidative addition of the P–C(acetylide) bond across a metal–metal edge. Compounds **1b**, **2b**, and **3b** have been structurally characterized by single-crystal X-ray analysis. Crystals of **1–3b** are monoclinic of space group $P2_1/n$ with unit cell dimensions. **1b**: a = 15.140 (3) Å, b = 10.559 (2) Å, c = 16.659 (3) Å, β = 110.61 (1)°. **2b**: a = 12.549 (1) Å, b = 14.528 (2) Å, c = 14.266 (1) Å, β = 92.95 (1)°. **3b**: a = 15.357 (2) Å, b = 10.604 (2) Å, c = 16.969 (2) Å, β = 111.56 (1)°. The structures were solved and refined to the following R and R_w values: **1b**, R = 0.028, R_w = 0.031 on 3071 observed ($I \geq 3\sigma(I)$) data; **2b**, R = 0.028, R_w = 0.030 on 4349 observed ($I \geq 3\sigma(I)$) data; **3b**, R = 0.035, R_w = 0.040 on 2734 observed ($I \geq 3\sigma(I)$) data. The three molecules are isostructural with a metal–metal bond supported by a phosphido bridge and a σ–π bound acetylide ligand. In solution all three compounds are fluxional via processes of acetylide σ–π interchange and $M(CO)_3$ trigonal rotation. Changes in structural parameters down the triad are discussed.

As a carbon ligand isoelectronic with both CO and CN^-, organometallic complexes of the acetylide anion $HC{\equiv}C^-$ have been known for decades.[1] In fact, acetylides are virtually unrivaled among unsaturated hydrocarbyls in

0276-7333/88/2307-0969$01.50/0

their ability to bond to transition metals not only as terminal ligands but also via a great variety of multisite interactions[2] including symmetrical μ_2, edge-bridging μ_2-η^2, and face-bridging μ_3-η^2 or μ_4-η^2 modes. Their unsaturation, coupled with susceptibility to both nucleophilic[3] and electrophilic[4] attack, make them attractive two-carbon fragments for the generation of other hydrocarbyls including vinyl, vinylidene, alkylidene, alkylidyne, and alkyl groups. Considerable progess has been made in recent years in understanding the reaction chemistry of terminal organometallic acetylides and the interrelationships between acetylides and other hydrocarbyls.[5] We have been interested in defining and exploiting the potential of multisite-bound alkynyl groups for organic transformations on polynuclear systems,[6] and we have completed an in-depth analysis of the binuclear μ_2-η^2-acetylides $M_2(CO)_6(\mu_2\text{-}\eta^2\text{-}C{\equiv}CR)(\mu\text{-}PPh_2)$ (M = Fe, Ru, Os; R = Ph, *t*-Bu, *i*-Pr) including synthesis, structural characterization, ^1H, ^{31}P, and ^{13}C NMR studies, and EHMO calculations coupled with reactivity patterns. In this the first of three papers we describe synthetic procedures, the X-ray structures of an entire triad of isostructural complexes **1b** (R = *t*-Bu, M = Fe), **2b** (R = *t*-Bu, M = Ru), and **3b** (R = *t*-Bu, M = Os), spectroscopic features, and some aspects of their dynamic behavior.

Experimental Section

General Procedures. All reactions were carried out under an atmosphere of dry nitrogen by using Schlenk techniques. Solvents were dried over the following solvents and distilled under nitrogen before use: benzene, THF (sodium benzophenone ketyl), heptane ($LiAlH_4$), methanol (CaO); CH_2Cl_2 (P_2O_5). Metal carbonyls, $M_3(CO)_{12}$ (M = Fe, Ru, Os), were purchased from Strem Chemicals. The phosphinoalkynes $Ph_2PC{\equiv}CR$ (R = Ph, *t*-Bu, *i*-Pr) were synthesized as previously described.[7] Trimethylamine *N*-oxide dihydrate was purchased from Aldrich Chemical Co. and was dehydrated prior to use by sublimation in vacuo. IR spectra were recorded in solution by using 0.5-mm NaCl cells, on a Perkin-Elmer 180 spectrometer. NMR spectra were measured on the following spectrometers: $^{31}P\{^1H\}$ spectra on a Bruker WP-80 instrument at 32.38 MHz (reference 85% H_3PO_4); ^1H at 80, 250, or 400 MHz on a Bruker WP-80, AM-250, or WH-400 instrument (reference TMS); $^{13}C\{^1H\}$ at 50.32 or 101.1 MHz on a Bruker AC-200 or on a Bruker WH 400 instrument (reference TMS). Elemental analyses were performed by Guelph Chemical Laboratories.

Syntheses

$Fe_2(CO)_6(\mu_2\text{-}\eta^2\text{-}C{\equiv}CPh)(\mu\text{-}PPh_2)$ (1a). Triiron dodecacarbonyl (2.00 g, 3.97 mmol) was stirred in *n*-heptane (100 mL) and benzene (230 mL) with excess (1.22 g, 4.25 mmol) $Ph_2PC{\equiv}CPh$ as a solution of Me_3NO (0.33 g) in methanol (15 mL) was added over a period of 2 h. The solution was stirred for an additional hour and contained mainly $Fe_3(CO)_{11}(Ph_2PC{\equiv}CPh)$ at this point. Heating at 70 °C for 2 h produced a brown-orange mixture. The solution was cooled to room temperature, concentrated to approximately 15 mL, and placed on a 30 cm × 5 cm Florisil heptane column and eluted with heptane. The first band was green and consisted of $Fe_3(CO)_{12}$. The second band was red-orange and contained **1a**. The third band was yellow [$Fe(CO)_4(Ph_2PC{\equiv}CPh)$] and ran into the last portion of the band containing **1a**. The first two thirds of the second band was concentrated to 5–10 mL and stored at −10 °C for 24 h. The isolated yield of red crystals of **1a** was 1.01 g (1.78 mmol, 41.6%). **1b** (17.2%) and **1c** (48.8%) were prepared in a similar fashion by using $Ph_2PC{\equiv}C$-*t*-Bu and $Ph_2PC{\equiv}C$-*i*-Pr in place of $Ph_2PC{\equiv}CPh$.

$Ru_2(CO)_6(\mu_2\text{-}\eta^2\text{-}C{\equiv}C\text{-}t\text{-}Bu)(\mu\text{-}PPh_2)$ (2b). Triruthenium dodecacarbonyl (2.00 g, 3.13 mmol) was dissolved in THF (300 mL). Excess (1.00 g, 3.75 mmol) $Ph_2PC{\equiv}C$-*t*-Bu in THF (25 mL) was added by syringe through a serum cap. A catalytic amount of sodium benzophenone ketyl[8] in THF was added to the orange solution which immediately turned dark red. The solution containing mainly $Ru_3(CO)_{11}(Ph_2PC{\equiv}C\text{-}t\text{-}Bu)$ was heated at 80 °C for 4 h. The solution was desolvated and dried onto Florisil. The stained Florisil was placed on top of a 30 cm × 5 cm fresh Florisil column and eluted with heptane. The first band (orange-yellow) was $Ru_3(CO)_{12}$. The second band (pale yellow) was **2b**. The eluant from this band was concentrated to 5–10 mL, a seed crystal added and the solution stored at −10 °C for 48 h. The isolated yield of yellow crystals was 1.61 g (2.53 mmol 67.4%). **2a** (47.9%) and **2c** (60.0%) were prepared in a similar fashion to **2b** by using $Ph_2PC{\equiv}CPh$ and $Ph_2PC{\equiv}C$-*i*-Pr.

$Os_2(CO)_6(\mu_2\text{-}\eta^2\text{-}C{\equiv}C\text{-}i\text{-}Pr)(\mu\text{-}PPh_2)$ (3c). The monosubstituted carbonyl $Os_3(CO)_{11}(Ph_2PC{\equiv}C$-*i*-Pr) (1.94 g) prepared from $Os_3(CO)_{11}(MeCN)$ and ligand by the Johnson and Lewis method[9] was sealed in a Carius tube in vacuo. The tube was heated at 205 °C for 20 min. The yellow solid melted to a dark red-brown liquid. The tube and its contents were cooled to room temperature and the tube was opened. The solids were mixed with methylene chloride, the mixture was filtered and the solids ($Os_3(CO)_{12}$) were washed with methylene chloride. The methylene chloride solution was desolvated and dried onto Florisil. The stained Florisil was placed on top of a fresh 30 cm × 5 cm Florisil column and eluted with heptane. The first band was pale yellow and was identified as $Os_3(CO)_{12}$. A pale orange color lead an almost colorless band of **3c**. The eluant of this band was concentrated to 0.5 mL, a seed crystal added and the solution stored at −10 °C for 24 h. The isolated yield of **3c**, pale yellow crystals, was 0.597 g (0.745 mmol, 43.6%). A third pale yellow band of $Os_3(CO)_9(\mu_3\text{-}\eta^2\text{-}C{\equiv}\text{-}C\text{-}i\text{-}Pr)(\mu\text{-}PPh_2)$[10] followed. **3a** (30%) and **3b** (63.7%) were synthesized in a similar manner using $Os_3(CO)_{11}(Ph_2PC{\equiv}CPh)$ and $Os_3(CO)_{11}(Ph_2PC{\equiv}C\text{-}t\text{-}Bu)$.

1a: IR (C_6H_{12}) ν(CO) 2072 s, 2035 vs, 2009 s, 1989 s, 1973 w cm^{-1}; $^{31}P\{^1H\}$ NMR (C_6D_6) δ +148.3; $^{13}C\{^1H\}$ NMR ($CDCl_3$) δ 209.9 (CO, s), 138.4 (C_i, d, $^1J_{P\text{-}C}$ = 25.0 Hz), 134.0 (C'_i, d, $^1J_{P\text{-}C}$ = 33.6 Hz), 134.0 (C_o, d, $^2J_{P\text{-}C}$ = 8.2 Hz), 132.9 (C'_o, d, $^2J_{P\text{-}C}$ = 8.2 Hz), 131.4 (C''_o, d, $^4J_{P\text{-}C}$ = 2.2 Hz), 129.8 (C_p, d, $^4J_{P\text{-}C}$ = 2.5 Hz), 129.4 (C'_p, d, $^4J_{P\text{-}C}$ = 3.2 Hz), 128.5 (C_m, d, $^3J_{P\text{-}C}$ = 9.4 Hz), 128.0 (C''_p,

(1) For a review of acetylide coordination chemistry see: Nast, R. *Coord. Chem. Rev.* **1982**, *47*, 89.

(2) (a) Carty, A. J. *Pure Appl. Chem.* **1982**, *54*, 113. (b) For a comparison of bonding modes for acetylides and related ligands on clusters see: Sappa, E.; Tiripicchio, A.; Braunstein, P. *Coord. Chem. Rev.* **1985**, *65*, 219.

(3) (a) Wong, Y. S.; Paik, H. N.; Chieh, P. C.; Carty, A. J. *J. Chem. Soc., Chem. Commun.* **1975**, 309. (b) Carty, A. J.; Taylor, N. J.; Paik, H. N.; Smith, W.; Yule, J. G. *J. Chem. Soc., Chem. Commun.* **1976**, 41. (c) Deeming, A. J.; Hasso, S. *J. Organomet. Chem.* **1976**, *112*, C39. (d) Churchill, M. R.; DeBoer, B. G.; Shapley, J. R.; Keister, J. B. *J. Am. Chem. Soc.* **1976**, *98*, 2357. (e) Henrick, K.; McPartlin, M.; Deeming, A. J.; Hasso, S.; Manning, P. *J. Chem. Soc., Dalton Trans.* **1982**, 899. (f) Mott, G. N.; Carty, A. J. *Inorg. Chem.* **1983**, *22*, 2726 and references therein.

(4) (a) Bell, R. A.; Chisholm, M. H. *Inorg. Chem.* **1977**, *16*, 687. (b) Bruce, M. I.; Swincer, A. G. *Adv. Organomet. Chem.* **1983**, *22*, 59 and references therein. (c) Bruce, M. I.; Wallis, R. C. *J. Organomet. Chem.* **1978**, *161*, C1. (d) Davison, A.; Selegue, J. P. *J. Am. Chem. Soc.* **1978**, *100*, 7763. (e) Berke, H. *Z. Naturforsch., B: Anorg. Chem., Org. Chem.* **1980**, *35B*, 86. (f) Carty, A. J.; Taylor, N. J.; Sappa, E.; Tiripicchio, A. *Inorg. Chem.* **1983**, *21*, 1871. (g) Hriljac, J. A., Shriver, D. F. *Organometallics* **1985**, *4*, 2225. (h) Mays, A.; Schaefer, K. C.; Huang, E. Y. *J. Am. Chem. Soc.* **1984**, *106*, 1517. (i) Sebald, A.; Wrackmeyer, B. *J. Chem. Soc., Chem. Commun.* **1983**, 1293.

(5) See ref 4 and also: Kostic, N. M.; Fenske, R. F. *Organometallics* **1982**, *1*, 974.

(6) (a) For an earlier review of our work in this area see: Fehlhammer, W. P.; Stolzenberg, H. In *Comprehensive Organometallic Chemistry*; Wilkinson, G., Stone, F. G. A., Abel, E. W., Eds.; Pergamon: Oxford, 1982; Vol. 4, Chapter 31, pp 513–613. (b) Nucciarone, D.; Taylor, N. J.; Carty, A. J. *Organometallics* **1984**, *3*, 177. (c) Nucciarone, D.; MacLaughlin, S. A.; Taylor, N. J.; Carty, A. J. *Organometallics* **1988**, *7*, 106.

(7) Carty, A. J.; Hota, N. K.; Ng, T. W.; Patel, H. A.; O'Connor, T. J. *Can. J. Chem.* **1971**, 2706.

(8) Bruce, M. I.; Kehoe, D. C.; Matisons, J. G.; Nicholson, B. K.; Rieger, P. H.; Williams, M. L. *J. Chem. Soc., Chem. Commun.* **1982**, 442.

(9) Johnson, B. F. G.; Lewis, J.; Pippard, D. A. *J. Chem. Soc., Dalton Trans.* **1981**, 407.

(10) Carty, A. J.; MacLaughlin, S. A.; Taylor, N. J. *J. Organomet. Chem.* **1981**, *204*, C27.

s), 127.9 (C''_m, s), 127.8 (C'_m, d, $^3J_{P-C}$ = 10.4 Hz), 125.7 (C''_i, d, $^3J_{P-C}$ = 3.0 Hz), 110.0 (C_α, d, $^2J_{P-C}$ = 52.9 Hz), 91.7 (C_β, d, $^2J_{P-C}$ = 7.7 Hz). Anal. Calcd for $Fe_2PO_6C_{26}H_{15}$: C, 55.17; H, 2.67; P, 5.47. Found: C, 55.07; H, 2.56; P, 5.35.

1b: IR (C_6H_{12}) ν(CO) 2072 s, 2032 vs, 2007 s, 1986 s, 1984 s, 1969 w cm^{-1}; $^{31}P\{^1H\}$ NMR (C_6D_6) δ +148.4; $^{13}C\{^1H\}$ NMR ($CDCl_3$) δ 210.5 (CO, s), 138.8 (C_i, d, $^1J_{P-C}$ = 25 Hz), 134.5 (C_o, d, $^2J_{P-C}$ = 7.6 Hz), 134.1 (C'_i, d, $^1J_{P-C}$ = 33.5 Hz), 133.1 (C'_o, d, $^2J_{P-C}$ = 8.0 Hz), 130.1 (C_p, d, $^4J_{P-C}$ = 2.4 Hz), 129.4 (C'_p, d, $^4J_{P-C}$ = 3.4 Hz), 128.5 (C_m, d, $^3J_{P-C}$ = 10.3 Hz), 127.5 (C'_m, d, $^3J_{P-C}$ = 10.6 Hz), 106.3 (C_β, d, $^2J_{P-C}$ = 8.0 Hz), 97.7 (C_α, d, $^2J_{P-C}$ = 53.4 Hz), 31.0 (CMe_3, d, $^3J_{P-C}$ = 2.3 Hz), 30.7 (CH_3, s). Anal. Calcd for $Fe_2PO_6C_{24}H_{19}$: C, 52.79; H, 3.64; P, 5.49. Found: C, 52.92; H, 3.51; P, 5.67.

1c: IR (C_6H_{12}) ν(CO) 2072 s, 2033 vs, 2008 s, 1986 s, 1969 w cm^{-1}; $^{31}P\{^1H\}$ NMR (C_6D_6) δ +149.7; $^{13}C\{^1H\}$ NMR ($CDCl_3$) δ 210.3 (CO, s), 138.7 (C_i, d, $^1J_{P-C}$ = 23.5 Hz), 134.4 (C'_i, d, $^1J_{P-C}$ = 33.1 Hz), 134.1 (C_o, d, $^2J_{P-C}$ = 7.7 Hz), 132.9 (C'_o, d, $^2J_{P-C}$ = 8.1 Hz), 130.1 (C_p, d, $^4J_{P-C}$ = 2.4 Hz), 129.3 (C'_p, d, $^4J_{P-C}$ = 3.2 Hz), 128.4 (C_m, d, $^3J_{P-C}$ = 9.3 Hz), 127.5 (C'_m, d, $^3J_{P-C}$ = 10.4 Hz), 101.0 (C_β, d, $^2J_{P-C}$ = 7.7 Hz), 98.2 (C_α, d, $^2J_{P-C}$ = 52.7 Hz), 25.5 ($CHMe_2$, d, $^3J_{P-C}$ = 3.3), 22.7 (CH_3, s). Anal. Calcd for $Fe_2PO_6C_{23}H_{17}$: C, 51.93; H, 3.22; P, 5.82. Found: C, 52.00; H, 3.24; P, 5.59.

2a: IR (C_6H_{12}) ν(CO) 2082 s, 2052 vs, 2018 vs, 2003 m sh, 1997 s, 1985 m cm^{-1}; $^{31}P\{^1H\}$ NMR (C_6D_6) δ +130.5; $^{13}C\{^1H\}$ NMR ($CDCl_3$) δ 197.4 (CO_a, d, $^2J_{P-C}$ = 11.7 Hz), 195.3 (CO_b, d, $^2J_{P-C}$ = 72.7 Hz), 194.0 (CO_c, d, $^2J_{P-C}$ = 6.1 Hz), 130.9 (C_i, d, $^1J_{P-C}$ = 28.5 Hz), 134.2 (C_o, d, $^2J_{P-C}$ = 9.7 Hz), 133.5 (C'_i, d, $^1J_{P-C}$ = 32.8 Hz), 133.0 (C'_o, d, $^2J_{P-C}$ = 10.2 Hz), 131.5 (C''_o, d, $^4J_{P-C}$ = 1.6 Hz), 129.8 (C_p, d, $^4J_{P-C}$ = 2.4 Hz), 129.1 (C'_p, d, $^4J_{P-C}$ = 2.8 Hz), 128.4 (C_m, d, $^3J_{P-C}$ = 10.0 Hz), 127.9 (C''_m, s), 127.9 (C'_m, d, $^3J_{P-C}$ = 10.4 Hz), 127.7 (C''_p, s), 126.8 (C''_i, d, $^3J_{P-C}$ = 2.5 Hz), 105.4 (C_α, d, $^2J_{P-C}$ = 27.5 Hz), 92.7 (C_β, d, 7.7 Hz). Anal. Calcd for $Ru_2PO_6C_{26}H_{15}$: C, 47.56; H, 2.30; P, 4.72. Found: C, 47.39; H, 2.35; P, 4.63.

2b: IR (C_6H_{12}) ν(CO) 2081 s, 2050 vs, 2016 vs, 1994 s, 1981 m cm^{-1}, $^{31}P\{^1H\}$ NMR (C_6D_6) δ +125.2; $^{13}C\{^1H\}$ NMR ($CDCl_3$) δ 197.5 (CO_a, d, $^2J_{P-C}$ = 12 Hz), 195.7 (CO_b, d, $^2J_{P-C}$ = 73.6 Hz), 194.8 (CO_c, d, $^2J_{P-C}$ = 6.1 Hz), 139.1 (C_i, d, $^1J_{P-C}$ = 29.4 Hz), 134.6 (C_o, d, $^2J_{P-C}$ = 9.7 Hz), 133.4 (C'_i, d, $^1J_{P-C}$ = 31.7 Hz), 133.3 (C'_o, d, $^2J_{P-C}$ = 10.2 Hz), 129.8 (C_p, d, $^4J_{P-C}$ = 2.4 Hz), 129.1 (C'_p, d, $^4J_{P-C}$ = 2.9 Hz), 128.3 (C_m, d, $^3J_{P-C}$ = 9.6 Hz), 127.5 (C'_m, d, $^3J_{P-C}$ = 10.5 Hz), 106.7 (C_β, d, $^2J_{P-C}$ = 7.8 Hz), 93.4 (C_α, d, $^2J_{P-C}$ = 27.8 Hz) 31.2 (CH_3, s), 30.9 (CMe_3, d, $^3J_{P-C}$ = 1.7 Hz). Anal. Calcd for $Ru_2PO_6C_{24}H_{19}$: C, 45.32; H, 3.01; P, 4.87. Found: C, 44.96; H, 3.00; P, 5.09.

2c: IR (C_6H_{12}) ν(CO) 2081 s, 2050 vs, 2016 vs, 1997 s, 1982 m cm^{-1}; $^{31}P\{^1H\}$ NMR (C_6D_6) δ +126.1; $^{13}C\{^1H\}$ NMR ($CDCl_3$) δ 197.5 (CO_a, d, $^2J_{P-C}$ = 12.0 Hz), 195.7 (CO_b, d, $^2J_{P-C}$ = 73.8 Hz), 194.5 (CO_c, d, $^2J_{P-C}$ = 5.8 Hz), 139.2 (C_i, d, $^1J_{P-C}$ = 28.0 Hz), 134.4 (C_o, d, $^2J_{P-C}$ = 9.6 Hz), 133.6 (C'_i, d, $^1J_{P-C}$ = 33.4 Hz), 133.1 (C'_o, d, $^2J_{P-C}$ = 10.2 Hz), 129.7 (C_p, d, $^4J_{P-C}$ = 3.0 Hz), 129.0 (C'_p, d, $^4J_{P-C}$ = 3.0 Hz), 128.3 (C_m, d, $^3J_{P-C}$ = 9.7 Hz), 127.6 (C'_m, d, $^3J_{P-C}$ = 10.6 Hz), 101.2 (C_β, d, $^2J_{P-C}$ = 8.0 Hz), 93.0 (C_α, d, $^2J_{P-C}$ = 27.4 Hz), 25.8 ($CHMe_2$, d, $^3J_{P-C}$ = 2.0 Hz), 23.4 (CH_3, s). Anal. Calcd for $Ru_2PO_6C_{23}H_{17}$: C, 44.0; H, 2.75. Found: C, 44.49; H, 2.71.

3a: IR (C_6H_{12}) ν(CO) 2081 s, 2051 vs, 2009 vs, 1989 s, 1978 m cm^{-1}; $^{31}P\{^1H\}$ NMR (C_6D_6) δ +47.3; $^{13}C\{^1H\}$ NMR ($CDCl_3$) δ 178.1 (CO_a, d, J_{P-C} = 8.1 Hz), 177.5 (CO_b, d, $^2J_{P-C}$ = 78.7 Hz); 175.1 (CO_c, d, 5.6 Hz), 136.5 (C_i, d, $^1J_{P-C}$ = 39.5 Hz), 135.1 (C_o, d, $^2J_{P-C}$ = 10.5 Hz), 133.7 (C'_o, d, $^2J_{P-C}$ = 10.6 Hz), 132.0 (C''_o, d, $^4J_{P-C}$ = 2.0 Hz), 130.4 (C_p, d, $^4J_{P-C}$ = 2.7 Hz), 129.5 (C'_p, d, $^4J_{P-C}$ = 2.8 Hz), 129.4 (C'_i, d, $^1J_{P-C}$ = 39.7 Hz), 128.8 (C_m, d, $^3J_{P-C}$ = 10.4 Hz), 128.3 (C'_m, d, $^3J_{P-C}$ = 10.9 Hz), 128.1 (C''_m, s), 128.0 (C''_p, s), 127.5 (C''_i, d, $^3J_{P-C}$ = 3.5 Hz), 90.4 (C_β, d, $^2J_{P-C}$ = 9.3 Hz), 86.0 (C_α, d, $^2J_{P-C}$ = 19.8 Hz). Anal. Calcd for $Os_2PO_6C_{26}H_{15}$: C, 37.41; H, 1.81; P, 3.71. Found: C, 37.44; H, 1.79; P, 3.62.

3b: IR (C_6H_{12}) ν(CO) 2079 s, 2048 vs, 2006 vs, 1984 s, 1974 m cm^{-1}; $^{31}P\{^1H\}$ NMR (C_6D_6) δ +45.3; $^{13}C\{^1H\}$ NMR ($CDCl_3$) δ 178.1 (CO_a, d, $^2J_{P-C}$ = 8.0 Hz), 177.7 (CO_b, d, $^2J_{P-C}$ = 69.3 Hz), 175.7 (CO_c, d, $^2J_{P-C}$ = 6.2 Hz), 136.8 (C_i, d, $^1J_{P-C}$ = 40.8 Hz), 135.5 (C_o, d, $^2J_{P-C}$ = 10.3 Hz), 134.1 (C'_o, d, $^2J_{P-C}$ = 10.6 Hz), 130.3 (C_p, d, $^4J_{P-C}$ = 2.5 Hz), 129.5 (C'_p, d, $^4J_{P-C}$ = 2.9 Hz), 121.1 (C'_i, d, $^1J_{P-C}$ = 38 Hz), 128.7 (C_m, d, $^3J_{P-C}$ = 10.4 Hz), 127.9 (C'_m, d, $^3J_{P-C}$ = 11.0 Hz), 103.7 (C_β, d, $^2J_{P-C}$ = 9.5 Hz), 73.1 (C_α, d, $^2J_{P-C}$ = 19.5 Hz), 32.2 (CMe_3, d, $^3J_{P-C}$ = 2.4 Hz), 31.2 (CH_3, d, $^4J_{P-C}$ = 1.2 Hz).

Table I. $^{13}C\{^1H\}$ Carbonyl and Methyl Group Shifts (δ) and ^1H Methyl Group Resonances (δ) for $M_2(CO)_6(\mu_2$-η^2-C≡C-*i*-Pr)(μ-PPh_2) at 293 and 193 K

		^{13}C (CO)		^{13}C (Me)	^1H (Me)
Fe	293 K	211.0 (s) (all CO's)		23.0 (s)	0.85 (d) $^3J_{P-H}$ = 6.9 Hz
	193 K	213.5 (d) $^2J_{P-C}$ = 21.5 Hz	(CO_a)	22.9 (s)	0.58 (br s)
		212.8 (d) $^2J_{P-C}$ = 7.0 Hz	(CO_c)	20.9 (s)	0.81 (br s)
		211.6 (d) $^2J_{P-C}$ = 19.9 Hz	(CO_a)		
		211.3 (s)	(CO_c)		
		210.7 (d) $^2J_{P-C}$ = 35.5 Hz	(CO_b)		
		208.1 (d) $^2J_{P-C}$ = 46.6 Hz	(CO_b)		
Ru	293 K	198.1 (d) $^2J_{P-C}$ = 12.0 Hz	(CO_a)	23.7 (s)	0.81 (d) $^3J_{P-H}$ = 6.9 Hz
		194.4 (d) $^2J_{P-C}$ = 73.8 Hz	(CO_b)		
		195.5 (d) $^2J_{P-C}$ = 5.8 Hz	(CO_c)		
	193 K	198.0 (d) $^2J_{P-C}$ = 11.6 Hz	(CO_a)	23.9 (s)	0.51 (d) $^3J_{P-H}$ = 6.4 Hz
		197.5 (d) $^2J_{P-C}$ = 10.0 Hz	(CO_a)	21.2 (s)	
		196.8 (d) $^2J_{P-C}$ = 70.3 Hz	(CO_b)		0.78 (d)
		195.2 (s)	(CO_c)		$^3J_{P-H}$ = 6.3 Hz
		194.8 (d) $^2J_{P-C}$ = 75.4 Hz	(CO_b)		
		193.5 (s)	(CO_c)		
Os	293 K	179.0 (br s)	(CO_a	23.8 (s)	0.84 (d)
		178.2 (d) $^2J_{P-C}$ = 69.1 Hz	(CO_b)		$^3J_{P-H}$ = 6.8 Hz
		175.8 (s) $^2J_{P-C}$ = 6.1 Hz	(CO_c)		
	193 K	180.1 (d) $^2J_{P-C}$ = 7.7 Hz	(CO_a)	24.1 (s)	0.61 (d)
		178.1 (d) $^2J_{P-C}$ = 63.8 Hz	(CO_b)	21.6 (s)	$^3J_{P-H}$ = 5.9 Hz
		177.3 (d) $^2J_{P-C}$ = 7.0 Hz	(CO_a)		0.75 (d)
		177.2 (d) $^2J_{P-C}$ = 74.2 Hz	(CO_b)		$^3J_{P-H}$ = 6.1 Hz
		176.4 (d) $^2J_{P-C}$ = 6.0 Hz	(CO_c)		
		174.0 (d) $^2J_{P-C}$ = 4.9 Hz	(CO_c)		

Anal. Calcd for $Os_2PO_6C_{24}H_{19}$: C, 35.38; H, 2.35; P, 3.80. Found: C, 35.24; H, 2.43; P, 3.81.

3c: IR (C_6H_{12}) ν(CO) 2080 s, 2048 vs, 2006 vs, 1985 s, 1974 m, cm^{-1}; $^{31}P\{^1H\}$ NMR (C_6D_6) δ +48.0; $^{13}C\{^1H\}$ NMR ($CDCl_3$) δ 178.2 (CO_a, br s), 177.5 (CO_b, d, $^2J_{P-C}$ = 69.1 Hz), 175.1 (CO_c, d, $^2J_{P-C}$ = 6.1 Hz), 136.6 (C_i, d, $^1J_{P-C}$ = 39.5 Hz), 134.9 (C_o, d, $^2J_{P-C}$ = 10.5 Hz), 133.5 (C'_o, d, $^2J_{P-C}$ = 10.5 Hz), 130.0 (C_p, d, $^4J_{P-C}$ = 2.5 Hz), 129.4 (C'_i, d, $^1J_{P-C}$ = 39.0 Hz), 129.2 (C'_p, d, $^4J_{P-C}$ = 2.9 Hz), 128.4 (C_m, d, $^3J_{P-C}$ = 10.4 Hz), 127.8 (C'_m, d, $^3J_{P-C}$ = 10.9 Hz), 97.2 (C_β, d, $^2J_{P-C}$ = 9.5 Hz), 72.5 (C_α, d, $^2J_{P-C}$ = 18.9 Hz), 26.9 ($CHMe_2$, d, $^3J_{P-C}$ = 2.5 Hz), 23.3 (CH_3, s). Anal. Calcd for $Os_2PO_6C_{23}H_{17}$: C, 34.50; H, 2.14; P, 3.87. Found: C, 34.69; H, 2.07; P, 3.82.

Table I provides $^{13}C\{^1H\}$ and ^1H NMR data for complexes **1c**, **2c**, and **3c** at temperatures of 293 K and 193 K. Supplementary Table S_1 contains full details of ^1H NMR spectra for **1b**, **1c**, **2b**, **2c**, **3b**, and **3c**.

X-ray Structural Analyses for 1b, 2b, and 3b. Collection and Reduction of X-ray Data. Red crystals of **1b** were grown from benzene/heptane at −10 °C. A suitable prism was glued to a glass fiber with epoxy cement, mounted in a goniometer head and centered on a Syntex $P2_1$ diffractometer. From polaroid rotation photographic data input to the Syntex autoindexing and cell refinement routines a monoclinic unit cell was identified. Cell constants were refined from the setting angles of 15 reflections well dispersed in reciprocal space. Subsequent checks of axial reflections revealed systematic absences of $h0l$ for $h + l = 2n + 1$ and $0k0$ for $k = 2n + 1$, consistent with the space group $P2_1/n$, a nonstandard setting of $P2_1/c$.

Pale yellow crystals of **2b** were obtained from concentrated heptane solutions at −10 °C as were crystals of **3b**. Examination of preliminary diffractometer data for **2b** and **3b** confirmed that both crystals belonged to the monoclinic system, space group $P2_1/n$. Subsequent cell refinement suggested that **1b** and **3b** but not **2b** were isomorphous. Crystal data and instrumental parameters for the collection of intensity data are given in Table II. All three data sets were collected at 295 ± 1 K on a Syntex $P2_1$ diffractometer using graphite-monochromated Mo Kα (λ = 0.710 69 Å) radiation and θ–2θ scans with a variable scan rate set

Table II. Crystallogrphic Data for $M_2(CO)_6(\mu_2\text{-}\eta^2\text{-}C{\equiv}C\text{-}t\text{-}Bu)(\mu\text{-}PPh_2)$ (1b, M = Fe; 2b, M = Ru; 3b, M = Os)

	1b	2b	3b
mol formula	$Fe_2PO_6C_{24}H_{19}$	$Ru_2PO_6C_{24}H_{19}$	$Os_2PO_6C_{24}H_{19}$
mol wt	546.08	636.53	814.79
cryst size, mm^3	0.28 × 0.33 × 0.34	0.28 × 0.30 × 0.30	sphere 0.13 ± 2
space group	$P2_1/n$	$P2_1/n$	$P2_1/n$
cell dimens			
a, Å	15.140 (3)	12.549 (1)	15.357 (2)
b, Å	10.559 (2)	14.528 (2)	10.604 (2)
c, Å	16.659 (3)	14.266 (1)	16.969 (2)
β, deg	110.61 (1)	92.95 (1)	111.56 (1)
V, $Å^3$	2492.7 (8)	2597.4 (5)	2570.0 (6)
Z	4	4	4
ρ_{measd} $g\cdot cm^{-3}$ (by flotatn)	1.46 (CCl_4/C_6H_{12})	1.62 ($CCl_4/C_2H_2Br_4$)	2.10 ($CCl_4/C_2H_2Br_4$)
ρ_{calcd} $g\cdot cm^{-3}$	1.455	1.628	2.106
monochromator		single-crystal graphite	
radiatn		Mo Kα (λ = 0.710 69 Å)	
2θ range, deg	3.2–50	3.2–56	3.2–48
scan type	θ–2θ	θ–2θ	θ–2θ
scan speed, deg min^{-1}	2.0–29.3	2.0–29.3	2.0–29.3
scan width	[2θ(Mo Kα_1) − 0.9°] to [2θ(Mo Kα_2) + 0.9°]	[2θ(Mo Kα_1) − 0.8°] to [2θ(Mo Kα_2) + 0.8°]	[2θ(Mo Kα_1) − 0.75°] to [2θ(Mo Kα_2) + 0.75°]
std	418, 600	545, 347	327, 600
std variatn	±2%	±2%	−2%
transmissn factors	0.57–0.76	0.63–0.77	0.32–0.43
octants data	$h,k,\pm l$	$h,k,\pm l$	$h,k,\pm l$
measd data	4578	6313	4063
obsd data ($I \geq 3\sigma(I)$)	3071	4349	2734
μ(Mo Kα), cm^{-1}	12.95	12.33	106.04
F(000)	1112	1256	1512
residual density, $e.Å^{-3}$	0.3	0.5	1.4
R_{iso}	0.087	0.088	0.062
R	0.028	0.028	0.035
R_w	0.031	0.030	0.040
w^{-1}	$2.4 - 0.09\lvert F_o\rvert + 0.0015\lvert F_o\rvert^2$	$1.9 - 0.0243\lvert F_o\rvert + 0.000\,29\lvert F_o\rvert^2$	$2.3 - 0.0216\lvert F_o\rvert + 0.000\,12\lvert F_o\rvert^2$
$[(\sum(\lvert F_o\rvert - \lvert F_c\rvert)^2/(NO - NV))^{1/2}]$	0.68	0.93	2.87

to optimize measurements of weak reflections. Background measurements, using the stationary crystal–stationary counter method, were made at the beginning and end of each scan. Two standard reflections monitored after every 100 intensity measurements showed no significant changes (±2%). Measured reflections were flagged as unobserved when $I \geq 3\sigma(I)$ where σ was derived from counting statistics. Lorentz and polarization corrections were applied to the three data sets. A spherical absorption correction was applied to the data for **3b**.

Solution and Refinement of Intensity Data. A Patterson synthesis for the iron compound readily yielded positions for the two metal atoms. Standard Fourier methods were used to locate the remaining atoms in the molecule. Full-matrix least-squares refinement of positional and isotropic thermal parameters gave an R value ($R = \sum||F_o| - |F_c||/\sum|F_o|$) of 0.087. Conversion to anisotropic coefficients for all non-hydrogen atoms and several further cycles of refinement gave R = 0.039. At this stage a difference Fourier map revealed the positions of all hydrogen atoms. In subsequent refinements to convergence, hydrogen atom positions and isotropic temperature coefficients were included. The function minimized in least-squares calculations was $\sum w(|F_o| - |F_c|)^2$. The weighted R value is defined as $R_w = [\sum w(|F_o| - |F_c|)^2/\sum w|F_o|^2]^{1/2}$, where the weights w, which optimize on moderate intensities, were taken from the program RANGER. Scattering factors were taken from ref 11a, and the corrections for anomalous dispersion by the metal atoms were applied. Scattering factors for hydrogen were taken from the data of Stewart et al.[11b] The final R and R_w values together with residual electron density maxima are given in Table II.

For the diosmium compound **3b** atomic positions were initially assigned from the coordinates for **1b**. Refinement proceeded smoothly confirming isomorphism for these two molecules. Hydrogen atoms were not included in the refinement of **3b**. For **2b**, the ruthenium and phosphorus positions were located in a Patterson map and remaining atoms by Fourier techniques. Hydrogen atoms were included and refined after refinement to convergence with all non-hydrogen atoms having anisotropic temperature coefficients. Final difference maps were featureless in all three cases.

All calculations were carried out on an IBM 4341 network in the University of Waterloo Computing Centre, using a package of programs already described.[12] Atomic positional parameters for **1b–3b** are listed in Tables III–V, respectively, while Table VI contains an appropriate selection of bond lengths and angles. Anisotropic thermal parameters (Tables S2–S4), remaining bond lengths and angles (Table S5), and structure factors (Tables S6–S8) have been deposited as supplementary material.

Results and Discussion

Syntheses. Compounds **1–3** are all produced by the fragmentation of $M_3(CO)_{11}(Ph_2PC{\equiv}CR)$ (M = Fe, Ru, Os; R = Ph, *t*-Bu, *i*-Pr), readily accessible via the substitution of a single carbonyl group in $M_3(CO)_{12}$ by $Ph_2PC{\equiv}CR$ in the presence of Me_3NO (M = Fe), $Na^+Ph_2CO^{\bullet-}$ (M = Ru), or MeCN (M = Os). These phosphine-substitution products have been fully characterized elsewhere[6c,10] including an X-ray structure for $Ru_3(CO)_{11}(Ph_2PC{\equiv}CPh)$.[10] The formation of **1–3** from $M_3(CO)_{11}(Ph_2PC{\equiv}CR)$ involves oxidative insertion into the P–C bond of the phosphinoalkyne and cluster fragmentation (eq 1).

$$M_3(CO)_{11}(Ph_2PC{\equiv}CR) \xrightarrow{\Delta} M_2(CO)_6(\mu_2\text{-}\eta^2\text{-}C{\equiv}CR)(\mu\text{-}PPh_2) \quad (1)$$

The conditions required to effect the fragmentation reflect the increasing strengths of the M–M and M–C bonds down the triad: 70 °C, 2 h, M = Fe; 80 °C, 4 h, M = Ru; 205 °C, 20 min, M = Os. Several lines of evidence suggest that these reactions proceed as indicated in Scheme I. (i) The iron complexes can also be synthesized from $Fe_2(CO)_9$,[13,14] and in the case of R = *t*-Bu an intermediate

(11) (a) *International Tables for X-ray Crystallography*; Kynoch: Birmingham, England, 1974; Vol. IV. (b) Stewart, R. F.; Davidson, E. R.; Simpson, W. T. *J. Chem. Phys.* **1965**, *42*, 3175.

(12) Carty, A. J.; Mott, G. N.; Taylor, N. J.; Yule, J. E. *J. Am. Chem. Soc.* **1978**, *100*, 3051.

Table III. Atomic Positions (Fractional ×10⁴) and Hydrogen Atom Thermal Parameters (×10³) for $Fe_2(CO)_6(\mu_2\text{-}\eta^2\text{-}C_2\text{-}t\text{-}Bu)(\mu_2\text{-}PPh_2)$ (1b)

A. Heavy Atoms

atom	x	y	z
Fe(1)	3994.3 (3)	2382.4 (4)	315.2 (2)
Fe(2)	2829.6 (3)	2028.7 (4)	1124.3 (2)
P	2441.3 (5)	2530.2 (7)	-253.2 (4)
O(1)	4421 (2)	1953 (3)	-1237 (2)
O(2)	4260 (2)	5134 (2)	421 (2)
O(3)	5844 (2)	1862 (3)	1637 (2)
O(4)	918 (2)	1676 (2)	1132 (2)
O(5)	2918 (2)	4688 (2)	1618 (1)
O(6)	4006 (2)	1284 (2)	2885 (1)
C(1)	4276 (2)	2111 (3)	-619 (2)
C(2)	4157 (2)	4070 (3)	368 (2)
C(3)	5133 (2)	2078 (3)	1137 (2)
C(4)	1671 (2)	1752 (3)	1137 (2)
C(5)	2889 (2)	3654 (3)	1414 (2)
C(6)	3564 (2)	1564 (3)	2212 (2)
C(7)	3558 (2)	792 (2)	567 (2)
C(8)	3085 (2)	-24 (2)	747 (2)
C(9)	2694 (2)	-1287 (3)	846 (2)
C(10)	1622 (3)	-1269 (4)	518 (4)
C(11)	3110 (5)	-1705 (5)	1784 (3)
C(12)	3011 (3)	-2217 (4)	295 (3)
C(13)	1750 (2)	1400 (2)	-1061 (2)
C(14)	772 (2)	1435 (3)	-1307 (2)
C(15)	221 (3)	586 (4)	-1908 (2)
C(16)	629 (3)	-292 (4)	-2266 (2)
C(17)	1594 (3)	-356 (4)	-2030 (2)
C(18)	2158 (2)	502 (3)	-1419 (2)
C(19)	1861 (2)	4023 (3)	-681 (2)
C(20)	1221 (2)	4575 (3)	-378 (2)
C(21)	748 (3)	5676 (3)	-749 (3)
C(22)	918 (3)	6217 (4)	-1416 (3)
C(23)	1576 (4)	5701 (4)	-1706 (3)
C(24)	2041 (3)	4596 (4)	-1346 (2)

B. Hydrogen Atoms

atom	x	y	z	U_{iso}, Å²
H(10A)	136 (4)	-97 (6)	-3 (4)	190 (23)
H(10B)	144 (3)	-74 (5)	93 (3)	155 (16)
H(10C)	138 (3)	-209 (4)	56 (3)	123 (15)
H(11A)	285 (3)	-247 (4)	182 (3)	135 (15)
H(11B)	269 (3)	-108 (4)	196 (3)	142 (22)
H(11C)	377 (4)	-170 (5)	193 (3)	172 (19)
H(12A)	276 (2)	-309 (3)	35 (2)	87 (10)
H(12B)	368 (3)	-225 (3)	56 (2)	112 (15)
H(12C)	269 (3)	-194 (4)	-34 (3)	154 (18)
H(14)	49 (2)	200 (3)	-102 (2)	96 (12)
H(15)	-47 (3)	65 (3)	-204 (2)	111 (13)
H(16)	21 (3)	-90 (4)	-271 (2)	115 (14)
H(17)	189 (3)	-101 (4)	-226 (2)	120 (15)
H(18)	287 (2)	43 (3)	-122 (2)	75 (10)
H(20)	112 (2)	426 (3)	12 (2)	86 (11)
H(21)	27 (3)	605 (4)	-52 (3)	133 (16)
H(22)	60 (3)	702 (4)	-168 (3)	125 (14)
H(23)	172 (3)	604 (4)	-215 (3)	131 (15)
H(24)	246 (3)	423 (4)	-156 (2)	114 (15)

binuclear π-phosphinoalkyne complex $(CO)_4Fe(Ph_2PC_2\text{-}t\text{-}Bu)Fe(CO)_4$ has been isolated and characterized by X-ray analysis.[15] This molecule smoothly converts to **1b** at 60 °C with P–C cleavage, loss of CO, and M–M bond formation. (ii) For M = Ru, under mild conditions (0 °C, 7 days), $M_3(CO)_{11}(Ph_2PC{\equiv}CR)$ is converted to $Ru_3(CO)_9(\mu_3\text{-}\eta^2\text{-}C{\equiv}CR)(\mu\text{-}PPh_2)$ in good yields.[6c] Similarly for M = Os, temperatures of 200 °C give $Os_3(CO)_9(\mu_3\text{-}\eta^2\text{-}C{\equiv}CR)(\mu\text{-}PPh_2)$ as the major product. These observations

Scheme I

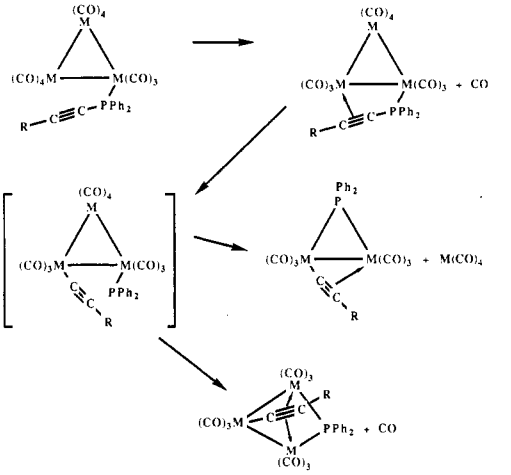

Scheme II

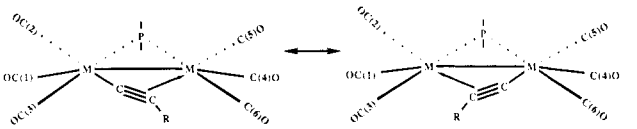

suggest that extrusion of an $M(CO)_n$ unit from a trinuclear species under conditions sufficiently rigorous to cause M–M bond scission is responsible for the synthesis of the binuclear compounds. (iii) In the related P-bound phosphinoalkyne complex $(\mu\text{-}H)Ru_3(CO)_9(\mu\text{-}PPh_2)(Ph_2PC{\equiv}CPh)$, intramolecular P–C activation at room temperature and hydride transfer to the generated acetylide lead to the formation of the bis(phosphido), alkyne complex $Ru_3(CO)_7(\mu_3\text{-}\eta^2\text{-}HC{\equiv}CPh)(\mu\text{-}PPh_2)_2$ in high yield. Thus it is clear that in these polynuclear systems $P\text{–}C_{sp}$ bond cleavage is a facile process,[16] phosphinoalkynes being a useful source of acetylides and phosphido groups.

Spectroscopic Studies. The IR ν(CO) spectra of **1–3** are typical of $M_2(CO)_6$ systems, with five distinct bands. Interestingly, frequencies increase in the order Fe < Os < Ru in any homologous series presumably reflecting greater π-back-bonding to CO in the iron complexes.

The ^{31}P chemical shifts are characteristic of $\mu\text{-}PPh_2$ groups across a strong iron triad metal–metal bond.[17] The upfield shifts of ~15 ppm between Fe and Ru and ~80 ppm between Ru and Os are entirely typical and can be used diagnostically to predict approximate shifts for related compounds within the triad.

Crystal structure analyses of **1b**, **2b**, and **3b** (vide infra) show that there are six chemically distinct carbonyl groups. However, in the carbon-13 NMR spectra of **1a–c** only a single carbonyl resonance is observed at 293 K. For complexes **2a–c** and **3a–c** three resonances are observed, each corresponding to two equivalent carbonyls. One of these peaks exhibits a large trans coupling to phosphorus (e.g., **2b**, $^2J_{P\text{-}C}$ = 73.8 Hz) while the other two exhibit smaller cis couplings (e.g., **2b**, $^2J_{P\text{-}C}$ = 12.0 Hz, $^2J_{P\text{-}C}$ = 5.8 Hz). These observations are explicable in terms of the occurrence at 293 K of a dynamic process involving $\sigma\text{–}\pi$ inter-

(13) Patel, H. A.; Fischer, R. G.; Carty, A. J.; Naik, D. V.; Palenik, G. J. *J. Organomet. Chem.* **1973**, *60*, C49.

(14) Smith, W. R.; Yule, J.; Taylor, N. J.; Paik, H. N.; Carty, A. J. *Inorg. Chem.* **1977**, *16*, 1593.

(15) Carty, A. J.; Smith, W. F.; Taylor, N. J. *J. Organomet. Chem.* **1978**, *146*, C1.

(16) (a) Van Gastel, F.; MacLaughlin, S. A.; Lynch, M.; Carty, A. J.; Sappa, E.; Tiripicchio, A.; Tiripicchio-Camellini, M. *J. Organomet. Chem.* **1987**, *326*, C65. (b) For an earlier review of P–C cleavage see: Garrou, P. E. *Chem. Rev.* **1985**, *85*, 171.

(17) (a) Carty, A. J. *Adv. Chem. Ser.* **1982**, *No. 196*, 163. (b) Carty, A. J.; MacLaughlin, S. A.; Nucciarone, D. In *Phosphorus-31 NMR Spectroscopy in Stereochemical Analysis: Organic Compounds and Metal Complexes*; Verkade, J. G., Quin, L. D., Eds.; VCH Publishers: New York, 1987; Chapter 16.

Table IV. Atomic Positions (Fractional ×10⁴) and Hydrogen Atom Thermal Parameters for $Ru_2(CO)_6(\mu_2\text{-}\eta^2\text{-}C_2\text{-}t\text{-}Bu)(\mu_2\text{-}PPh_2)$ (2b)

A. Heavy Atoms

atom	x	y	z
Ru(1)	1011.5 (2)	1391.3 (2)	1841.1 (2)
Ru(2)	-1122.1 (2)	1403.0 (2)	2201.5 (2)
P	-127.5 (6)	2665.8 (6)	1722.2 (5)
O(1)	3231 (2)	2205 (2)	2150 (2)
O(2)	1035 (3)	1172 (2)	-287 (2)
O(3)	1411 (3)	-657 (2)	2272 (3)
O(4)	-3238 (2)	2296 (2)	2646 (3)
O(5)	-1801 (3)	972 (3)	194 (2)
O(6)	-1396 (3)	-610 (2)	2824 (3)
C(1)	2421 (3)	1892 (3)	2027 (2)
C(2)	1051 (3)	1258 (3)	495 (3)
C(3)	1293 (4)	98 (3)	2098 (3)
C(4)	-2450 (3)	1964 (2)	2523 (3)
C(5)	-1555 (3)	1137 (3)	945 (3)
C(6)	-1323 (3)	125 (3)	2585 (3)
C(7)	406 (2)	1493 (2)	3140 (2)
C(8)	-243 (3)	1626 (2)	3732 (2)
C(9)	-659 (3)	1851 (3)	4673 (2)
C(10)	312 (4)	1977 (5)	5347 (3)
C(11)	-1357 (5)	1064 (4)	5000 (4)
C(12)	-1301 (4)	2734 (4)	4627 (3)
C(13)	33 (2)	3637 (2)	2527 (2)
C(14)	949 (3)	3783 (2)	3075 (2)
C(15)	1022 (4)	4538 (3)	3690 (3)
C(16)	191 (4)	5130 (3)	3742 (3)
C(17)	-719 (4)	4992 (3)	3199 (3)
C(18)	-799 (3)	4253 (3)	2593 (2)
C(19)	-450 (3)	3230 (2)	605 (2)
C(20)	-1495 (3)	3378 (3)	286 (3)
C(21)	-1709 (4)	3846 (3)	-556 (3)
C(22)	-900 (4)	4164 (3)	-1066 (3)
C(23)	130 (4)	4016 (3)	-760 (3)
C(24)	364 (3)	3554 (3)	78 (3)

B. Hydrogen Atoms

atom	x	y	z	U_{iso}, Å²
H(10A)	4 (4)	208 (3)	601 (3)	104 (18)
H(10B)	69 (4)	248 (3)	520 (3)	101 (16)
H(10C)	61 (5)	141 (4)	540 (4)	139 (19)
H(11A)	-193 (3)	91 (3)	453 (3)	73 (14)
H(11B)	-94 (4)	55 (3)	509 (3)	99 (15)
H(11C)	-158 (4)	126 (3)	561 (3)	98 (16)
H(12A)	-192 (4)	264 (4)	424 (4)	113 (18)
H(12B)	-100 (4)	321 (4)	442 (3)	101 (15)
H(12C)	-149 (3)	287 (3)	523 (3)	73 (11)
H(14)	149 (3)	337 (2)	304 (2)	50 (10)
H(15)	165 (3)	459 (3)	403 (3)	74 (14)
H(16)	38 (3)	563 (3)	419 (3)	93 (13)
H(17)	-131 (3)	535 (3)	327 (3)	82 (15)
H(18)	-137 (3)	414 (2)	228 (2)	54 (10)
H(20)	-207 (3)	314 (3)	67 (3)	71 (10)
H(21)	-243 (4)	392 (3)	-71 (3)	86 (13)
H(22)	-106 (4)	454 (4)	-159 (4)	115 (19)
H(23)	68 (4)	423 (4)	-103 (4)	127 (20)
H(24)	112 (3)	337 (3)	36 (3)	81 (13)

change of the acetylide between the two metals as shown in Scheme II, which equilibrates the two sides of the molecule [i.e. C(1)O and C(4)O, (CO_a); C(2)O and C(5)O, (CO_c); C(3)O and C(6)O, (CO_b)]. In addition in the case of iron, trigonal rotation of the carbonyls about the metal atoms equilibrates all of the carbonyls, resulting in one resonance only. Futher indication of the dynamic behavior of the acetylide is observed in the ^1H and ^{13}C NMR spectra of **1c**, **2c**, and **3c** (Table I) in which only one methyl isopropyl resonance is observed at 293 K, while a static structure would have two diastereotropic methyl groups. Table I also shows that at 193 K the static structures, with six chemically distinct carbonyl groups, are frozen out, indicating that acetylide fluxionality is slow on the NMR time scale. Assignments follow from the magnitudes of

Table V. Atomic Positions (Fractional ×10⁴) for $Os_2(CO)_6(\mu_2\text{-}\eta^2\text{-}C_2\text{-}t\text{-}Bu)(\mu_2\text{-}PPh_2)$ (3b)

atom	x	y	z
Os(1)	4014.1 (3)	2355.0 (4)	286.3 (3)
Os(2)	2761.3 (3)	2033.1 (4)	1118.9 (3)
P	2370 (2)	2525 (3)	-328 (2)
O(1)	4523 (8)	1909 (12)	-1258 (7)
O(2)	4241 (8)	5203 (9)	367 (8)
O(3)	5942 (8)	1887 (13)	1678 (8)
O(4)	847 (7)	1608 (10)	1210 (8)
O(5)	2789 (8)	4783 (8)	1603 (6)
O(6)	4024 (8)	1270 (10)	2923 (7)
C(1)	4360 (9)	2083 (12)	-669 (8)
C(2)	4160 (9)	4143 (12)	302 (9)
C(3)	5225 (10)	2057 (13)	1163 (10)
C(4)	1578 (9)	1702 (11)	1175 (8)
C(5)	2767 (9)	3737 (12)	1412 (8)
C(6)	3553 (9)	1567 (13)	2246 (8)
C(7)	3528 (8)	671 (11)	531 (7)
C(8)	3000 (9)	-44 (11)	711 (7)
C(9)	2570 (9)	-1279 (11)	767 (9)
C(10)	1513 (11)	-1228 (15)	387 (13)
C(11)	2941 (17)	-1707 (16)	1731 (10)
C(12)	2932 (11)	-2248 (12)	283 (11)
C(13)	1692 (9)	1414 (11)	-1140 (7)
C(14)	725 (9)	1403 (13)	-1381 (9)
C(15)	165 (11)	589 (15)	-1998 (12)
C(16)	561 (13)	-280 (15)	-2352 (9)
C(17)	1545 (13)	-308 (16)	-2113 (9)
C(18)	2140 (11)	542 (14)	-1479 (9)
C(19)	1816 (9)	4006 (11)	-752 (8)
C(20)	1145 (9)	4517 (12)	-467 (10)
C(21)	684 (11)	5661 (15)	-864 (12)
C(22)	916 (13)	6248 (15)	-1471 (11)
C(23)	1610 (15)	5761 (15)	-1716 (10)
C(24)	2066 (13)	4636 (14)	-1381 (9)

$^2J_{P\text{-}C}$ and from 2D (^{13}C–^{13}C) NOESY chemical exchange experiments to be described elsewhere.[18] On the basis of the coalescence temperatures of the diastereotopic methyl groups for **1c**, **2c**, and **3c** (213, 238, and 235 K, respectively), observed in the variable-temperature ^1H NMR spectra and using the approximate method[19] to determine kinetic parameters for the acetylide exchange process, values of $\Delta G^{\ddagger}$ for **1c**, **2c**, and **3c** are as follows: **1c**, 10.3 kcal mol^{-1}; **2c**, 11.2 kcal mol^{-1}; **3c**, 11.3 kcal mol^{-1}. These values lie in the normal range for fluxional processes involving edge-bridging hydrocarbyls on bi- or polynuclear frameworks. For comparison, Shapely et al.[20] reported $\Delta G^{\ddagger}$ of 10.3 kcal mol^{-1} in the σ-π-vinyl complex $(\mu\text{-H})Os_3(CO)_{10}(\mu_2\text{-}\eta^2\text{-CH=CH}_2)$, and Brown and co-workers[21] estimated a $\Delta G^{\ddagger}$ by the approximate method of 10.5 kcal mol^{-1} for $(\mu\text{-H})Re_2(CO)_6(\mu\text{-dppm})(\mu_2\text{-}\eta^2\text{-}C_2H)$. Since the series of compounds **1–3** represent the first complete triads of μ_2-η^2-bound acetylides, we have carried out a detailed analysis of their variable-temperature ^1H and ^{13}C spectra to extract accurate information on changes in $\Delta G^{\ddagger}$ as a function of metal. Full mechanistic details on the exchange process will be the subject of a forthcoming paper.[18]

The ^{13}C chemical shifts of the acetylide carbon atoms are of interest not only for diagnostic purposes and for comparison with shifts for other types of μ_n–η^2-acetylides but also for information which such shifts might provide

(18) Randall, L.; Cherkas, A. A.; Carty, A. J., submitted for publication.

(19) Free energies of activation were obtained by using the approximate equation $\Delta G^{\ddagger} = 4.576T_c[9.97 + \log T_c/\Delta\nu]$. $\Delta\nu$ = 92.7 Hz, 105.0 Hz, and 54.6 Hz for **1c**, **2c**, and **3c**, respectively. See: Kost, D.; Carlson, E. H.; Raban, M. *J. Chem. Soc., Chem. Commun.* **1971**, 656.

(20) (a) Shapley, J. R.; Richter, S. I.; Tachikawa, M.; Keister, J. B. *J. Organomet. Chem.* **1975**, *94*, C43. (b) Clauss, A. D.; Tachikawa, M.; Shapley, J. R.; Pierpont, C. G. *Inorg. Chem.* **1981**, *20*, 1528.

(21) Lee, K. W.; Pennington, W. T.; Cordes, A. W.; Brown, T. L. *J. Am. Chem. Soc.* **1985**, *107*, 631.

Table VI. Selected Bond Lengths (Å) and Angles (deg) for $M_2(CO)_6(\mu_2\text{-}\eta^2\text{-}C_2\text{-}t\text{-}Bu)(\mu_2\text{-}PPh_2)$ (M = Fe, 1b; M = Ru, 2b; M = Os, 3b)

	M = Fe	M = Ru	M = Os		M = Fe	M = Ru	M = Os
			A. Bond Lengths				
M(1)-M(2)	2.5959 (6)	2.7523 (3)	2.7950 (6)	P-C(19)	1.823 (3)	1.819 (3)	1.805 (12)
M(1)-P	2.2095 (8)	2.3399 (8)	2.359 (3)	C(1)-O(1)	1.137 (4)	1.119 (5)	1.132 (18)
M(1)-C(1)	1.776 (3)	1.918 (4)	1.904 (14)	C(2)-O(2)	1.133 (4)	1.123 (5)	1.132 (16)
M(1)-C(2)	1.797 (3)	1.933 (4)	1.908 (13)	C(3)-O(3)	1.128 (5)	1.132 (5)	1.141 (20)
M(1)-C(3)	1.813 (3)	1.943 (4)	1.933 (16)	C(4)-O(4)	1.140 (4)	1.123 (5)	1.150 (19)
M(1)-C(7)	1.905 (3)	2.044 (3)	2.036 (12)	C(5)-O(5)	1.140 (4)	1.126 (5)	1.152 (16)
M(2)-P	2.2231 (7)	2.3406 (8)	2.362 (3)	C(6)-O(6)	1.124 (4)	1.126 (5)	1.153 (17)
M(2)-C(4)	1.785 (3)	1.931 (4)	1.887 (15)	C(7)-C(8)	1.223 (4)	1.218 (4)	1.228 (18)
M(2)-C(5)	1.777 (3)	1.886 (4)	1.873 (13)	C(8)-C(9)	1.492 (4)	1.502 (4)	1.485 (17)
M(2)-C(6)	1.829 (3)	1.955 (4)	1.916 (13)	C(9)-C(10)	1.519 (6)	1.523 (6)	1.512 (24)
M(2)-C(7)	2.123 (3)	2.285 (3)	2.310 (12)	C(9)-C(11)	1.530 (6)	1.527 (7)	1.588 (21)
M(2)-C(8)	2.326 (3)	2.417 (3)	2.377 (12)	C(9)-C(12)	1.533 (5)	1.514 (7)	1.541 (21)
P-C(13)	1.828 (3)	1.824 (3)	1.821 (12)				
			B. Bond Angles				
M(2)-M(1)-P	54.40 (2)	54.00 (1)	53.75 (7)	C(5)-M(2)-C(6)	92.0 (1)	92.1 (1)	92.5 (5)
M(2)-M(1)-C(1)	148.0 (1)	150.6 (1)	150.6 (4)	C(5)-M(2)-C(7)	136.8 (1)	139.5 (1)	139.9 (4)
M(2)-M(1)-C(2)	102.9 (1)	105.1 (1)	102.3 (4)	C(5)-M(2)-C(8)	167.4 (1)	169.1 (1)	170.0 (4)
M(2)-M(1)-C(3)	102.8 (1)	98.0 (1)	103.7 (4)	C(6)-M(2)-C(7)	92.3 (1)	90.4 (1)	91.9 (5)
M(2)-M(1)-C(7)	53.7 (1)	54.5 (1)	54.4 (3)	C(6)-M(2)-C(8)	85.2 (1)	86.2 (1)	86.7 (5)
P-M(1)-C(1)	100.5 (1)	105.4 (1)	102.9 (4)	C(7)-M(2)-C(8)	31.5 (1)	29.8 (1)	30.3 (4)
P-M(1)-C(2)	93.3 (1)	93.1 (1)	91.8 (4)	M(1)-P-M(2)	71.70 (2)	72.03 (1)	72.61 (7)
P-M(1)-C(3)	157.2 (1)	152.0 (1)	157.5 (4)	M(1)-P-C(13)	121.1 (1)	121.3 (1)	120.0 (3)
P-M(1)-C(7)	76.0 (1)	75.8 (1)	75.2 (3)	M(1)-P-C(19)	121.5 (1)	121.8 (1)	120.6 (4)
C(1)-M(1)-C(2)	97.6 (1)	96.0 (1)	95.4 (5)	M(2)-P-C(13)	118.6 (1)	117.8 (1)	120.4 (3)
C(1)-M(1)-C(3)	100.1 (1)	100.6 (1)	98.0 (6)	M(2)-P-C(19)	121.7 (1)	120.7 (1)	120.9 (4)
C(1)-M(1)-C(7)	105.0 (1)	103.0 (1)	106.1 (5)	C(13)-P-C(19)	101.8 (1)	102.4 (1)	102.0 (5)
C(2)-M(1)-C(3)	93.5 (1)	94.4 (1)	94.4 (6)	M(1)-C(1)-O(1)	177.3 (1)	177.9 (1)	176.8 (6)
C(2)-M(1)-C(7)	156.4 (1)	159.6 (1)	156.7 (5)	M(1)-C(2)-O(2)	178.3 (1)	177.5 (1)	175.0 (6)
C(3)-M(1)-C(7)	89.4 (1)	88.3 (1)	91.2 (5)	M(1)-C(3)-O(3)	178.2 (1)	176.6 (1)	179.6 (6)
M(1)-M(2)-P	53.91 (2)	53.97 (1)	53.64 (7)	M(2)-C(4)-O(4)	174.5 (1)	175.3 (1)	174.2 (5)
M(1)-M(2)-C(4)	151.5 (1)	155.0 (1)	154.5 (3)	M(2)-C(5)-O(5)	178.0 (1)	179.0 (1)	178.6 (5)
M(1)-M(2)-C(5)	91.3 (1)	93.3 (1)	94.6 (3)	M(2)-C(6)-O(6)	179.1 (1)	177.1 (1)	179.1 (5)
M(1)-M(2)-C(6)	105.4 (1)	100.8 (1)	103.6 (4)	M(1)-C(7)-M(2)	80.1 (1)	78.7 (1)	79.8 (1)
M(1)-M(2)-C(7)	46.3 (1)	46.8 (1)	45.8 (3)	M(1)-C(7)-C(8)	162.4 (1)	158.9 (1)	156.5 (5)
M(1)-M(2)-C(8)	77.6 (1)	76.5 (1)	76.0 (3)	M(2)-C(7)-C(8)	83.5 (1)	81.1 (1)	77.9 (5)
P-M(2)-C(4)	98.4 (1)	102.6 (1)	102.2 (4)	M(2)-C(8)-C(7)	65.0 (1)	69.1 (1)	71.8 (5)
P-M(2)-C(5)	91.1 (1)	90.8 (1)	92.2 (4)	M(2)-C(8)-C(9)	133.9 (1)	132.3 (1)	132.7 (5)
P-M(2)-C(6)	159.2 (1)	154.7 (1)	157.0 (4)	C(7)-C(8)-C(9)	161.1 (1)	158.5 (2)	155.5 (7)
P-M(2)-C(7)	71.6 (1)	71.5 (1)	70.4 (3)	C(8)-C(9)-C(10)	111.4 (2)	106.7 (2)	112.0 (8)
P-M(2)-C(8)	87.2 (1)	86.2 (1)	84.8 (3)	C(8)-C(9)-C(11)	109.5 (2)	109.9 (2)	108.6 (8)
C(4)-M(2)-C(5)	96.4 (1)	95.8 (1)	94.4 (5)	C(8)-C(9)-C(12)	106.6 (1)	110.8 (2)	107.3 (7)
C(4)-M(2)-C(6)	101.6 (1)	102.1 (1)	99.8 (5)	C(10)-C(9)-C(11)	112.1 (3)	110.5 (3)	111.8 (10)
C(4)-M(2)-C(7)	124.6 (1)	123.0 (1)	124.0 (4)	C(10)-C(9)-C(12)	108.2 (2)	109.4 (2)	109.8 (9)
C(4)-M(2)-C(8)	96.2 (1)	95.1 (1)	95.5 (5)	C(11)-C(9)-C(12)	108.9 (2)	109.6 (2)	107.1 (9)

on charge density and polarization within the acetylide down the triad. Theoretical studies[22] suggest that the sum of the chemical shifts for acetylenic carbon atoms $\delta(C_\alpha) + \delta(C_\beta)$ provides an indication of total charge density on the triple bond while $\delta(C_\alpha) - \delta(C_\beta)$ is an indication of polarization of the bond. Table VII has these values for the nine compounds reported here. The ^{13}C acetylide resonances lie in the range 72.5–110.0 ppm downfield of TMS with C_α upfield of C_β in each case except for **1a** and **2a**. Since this pattern of chemical shift positions is opposite to that observed for $\mu_3\text{-}\eta^2$-bound acetylides,[4f,23] we performed a series of decoupling experiments to unequivocally assign these resonances. The ^{13}C NMR spectrum of **2c**, recorded under broad-band proton-noise decoupling, consists of two doublets, as shown in Figure 1A. Under

Table VII. Carbon-13 Chemical Shifts, Sums $[\delta(C_\alpha) + \delta(C_\beta)]$ and Differences $[\delta(C_\alpha) - \delta(C_\beta)]$, for Compounds $M_2(CO)_6(\mu_2\text{-}\eta^2\text{-}C{\equiv}CR)(\mu\text{-}PPh_2)$ (M = Fe, Ru, Os; R = Ph, *t*-Bu, *i*-Pr)

M	R	$C_\alpha + C_\beta$	$C_\alpha - C_\beta$
Fe	Ph	110.0 + 91.7 = 201.7	18.3
	t-Bu	97.7 + 106.3 = 204.0	−8.6
	i-Pr	98.2 + 101.0 = 199.2	−2.8
Ru	Ph	105.4 + 92.7 = 198.1	12.7
	t-Bu	93.4 + 106.7 = 200.1	−13.3
	i-Pr	93.0 + 101.2 = 194.2	−8.2
Os	Ph	86.0 + 90.4 = 176.4	−4.4
	t-Bu	73.1 + 103.7 = 176.8	−30.6
	i-Pr	72.5 + 97.2 = 169.7	−24.7

conditions of full proton coupling (Figure 1B) the lower field resonance consists of a doublet of doublets of septets ($^2J_{PC}$ = 8.0 Hz, $^2J_{CH}$ = 3.0 Hz, $^3J_{CH}$ = 3.2 Hz) which indicates that the β-carbon is coupled to both the methine proton and the methyl protons whereas the α-carbon is coupled only to the methine proton (doublet of doublets, $^2J_{PC}$ = 27.4 Hz, $^3J_{CH}$ = 5.0 Hz). These coupling patterns have been established by irradiation at the frequence of the methine proton (Figure 1C) and at the methyl resonance (not shown).

For each metal there is relatively little variation in total charge density with group R on the acetylide, but in each

(22) (a) Rosenberg, D.; Drenth, W. *Tetrahedron* **1971**, *27*, 3893. (b) Hagens, W.; Bos, H. J. T.; Arens, J. F. *Recl. Trav. Chim. Pays-Bas.* **1973**, *92*, 762. (c) Dawson, D. A.; Reynolds, W. F. *Can. J. Chem.* **1975**, *53*, 373. (d) Pople, J. A.; Gordon, M. *J. Am. Chem. Soc.* **1967**, *89*, 4253. (e) Sichel, J. M.; Whitehead, M. A. *Theor. Chim. Acta* **1966**, *5*, 35.

(23) (a) De Montauzon, D.; Mathieu, R. *J. Organomet. Chem.* **1983**, *252*, C83. (b) Green, M.; Marsden, K.; Salter, I. D.; Stone, F. G. A.; Woodward, P. *J. Chem. Soc., Chem. Commun.* **1983**, 446. (c) Aime, S.; Gambino, O.; Milone, L.; Sappa, E.; Rosenberg, E. *Inorg. Chim. Acta* **1975**, *15*, 53. For reviews see ref 2b and also: Mann, B. E. *Adv. Organomet. Chem.* **1974**, *12*, 135.

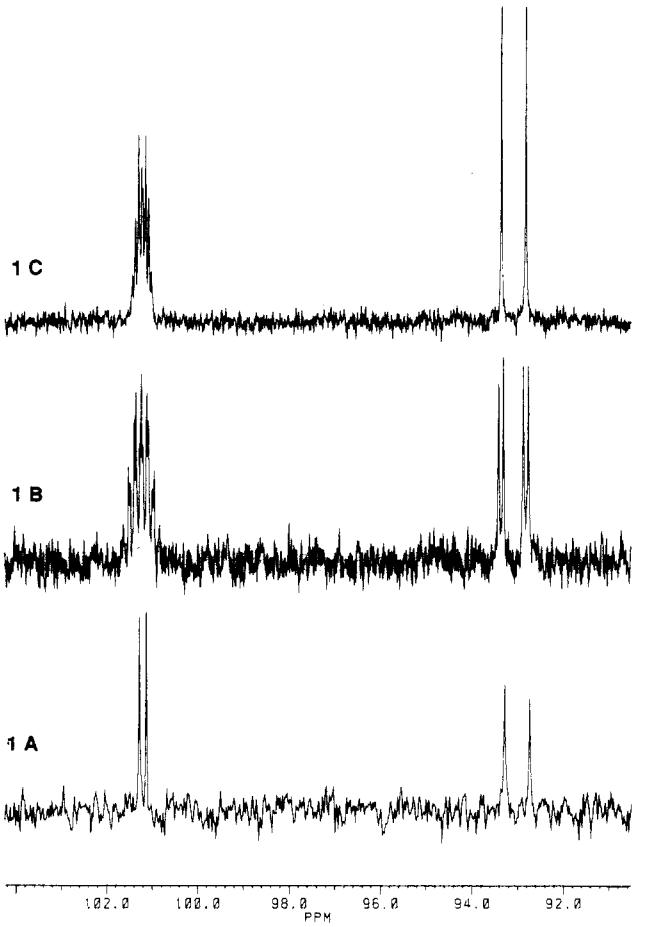

Figure 1. Carbon-13 NMR spectra of the acetylenic carbons of **2b** under conditions of (A) broad-band decoupling, (B) gated decoupling (fully proton coupled with NOE), and (C) selective proton decoupling (irradiation at the frequency of the methine proton, C*H*Me$_2$).

series the compound with R = *t*-Bu has the largest $\delta(C_\alpha) + \delta(C_\beta)$ as might be expected. A change from Fe to Ru produces a slightly smaller (less positive) sum, while from Ru to Os a significant drop in $\delta(C_\alpha) + \delta(C_\beta)$ occurs. Thus the diosmium compounds appear to carry more electron density on the acetylidic carbon atoms.

The polarization of the acetylide also changes with the metal and the R group. C_β becomes more positively charged ($[\delta(C_\alpha) - \delta(C_\beta)]$ becomes more negative) in the order Ph < *i*-Pr < *t*-Bu, consistent with theoretical calculations which suggest that the substituent on C_β principally affects the charge on C_α. When R = Ph, it is also noted that for M = Fe and Ru, C_α has the positive dipole of the acetylide while in the case of M = Os the polarity is reversed. For any particular R group the positive charge density on C_β increases in the order Fe < Ru < Os.

Structural Systematics in the Series 1b, 2b, and 3b. Complexes **1b**, **2b**, and **3b** are isostructural; **1b** and **3b** are isomorphous in the crystal. For conciseness and simplicity only the structure of **2b** (Figure 2) is illustrated. The same atomic numbering scheme is appropriate for **1b** and **3b**. A perspective view of the stereochemistry of the M_2PC_2 core is shown in Figure 3. Bond lengths and angles for all three molecules are tabulated in Table VI. For convenience of discussion of trends in molecular parameters down the triad Table VIII displays structural features of importance.

The two metal atoms are bonded by a strong metal–metal interaction, by the phosphorus atom of a bridging phosphido group, and by the alkynyl moiety which is σ-bound to M(1) and η^2-coordinated to M(2). The M(1)–M(2) bond lengths which, as expected due to the increasing atomic radius, lengthen down the triad are at the short end of the ranges expected for single bonds between these

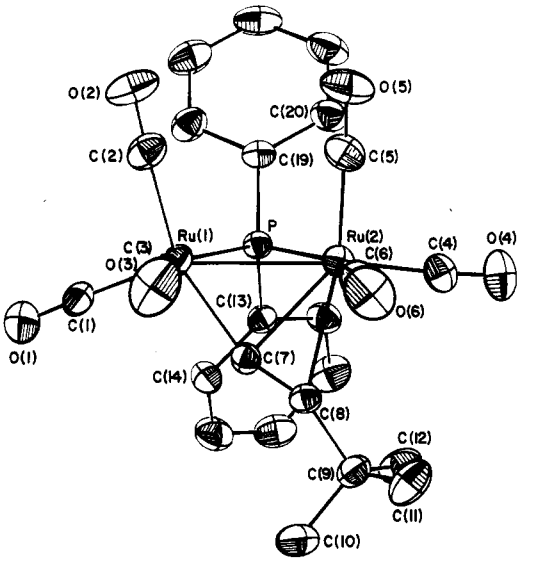

Figure 2. A perspective view of the molecular structure of $Ru_2(CO)_6(\mu_2\text{-}\eta^2\text{-}C{\equiv}C\text{-}t\text{-}Bu)(\mu\text{-}PPh_2)$ showing the atomic numbering. The labeling scheme is identical for the iron compound **1b** and the osmium complex **3b**.

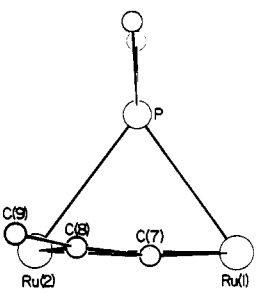

Figure 3. The stereochemistry of the M_2PC_2 core of $Ru_2(CO)_6(\mu_2\text{-}\eta^2\text{-}C{\equiv}C\text{-}t\text{-}Bu)(\mu\text{-}PPh_2)$ (**2b**).

Table VIII. Changes in Important Structural Parameters for the Series $M_2(CO)_6(\mu\text{-}PPh_2)(\mu_2\text{-}\eta^2\text{-}C{\equiv}C\text{-}t\text{-}Bu)$ (1b–3b)

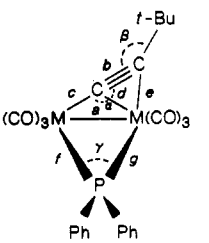

	M		
dist, Å	Fe	Ru	Os
a	2.5959 (6)	2.7523 (3)	2.7950 (6)
b	1.223 (4)	1.218 (4)	1.228 (18)
c	1.905 (3)	2.044 (3)	2.036 (12)
d	2.123 (3)	2.285 (3)	2.310 (12)
e	2.326 (3)	2.417 (3)	2.377 (12)
f	2.2095 (8)	2.3399 (8)	2.359 (3)
g	2.2231 (7)	2.3406 (8)	2.362 (3)
	M		
angle, deg	Fe	Ru	Os
α	162.4 (1)	158.9 (1)	156.6 (5)
β	161.1 (1)	158.5 (2)	155.5 (7)
γ	71.70 (2)	72.03 (1)	72.61 (7)

atoms.[24] For comparison the Fe(1)–Fe(2) distance in **1b** is similar to that in $Fe_2(CO)_6(\mu\text{-}Cl)(\mu\text{-}PPh_2)$ (2.5607 (5) Å),[25] in **2b** Ru(1)–Ru(2) is comparable to that in $Ru_2(CO)_6(\mu_2\text{-}O{=}CCHC(Ph)NEt_2)(\mu\text{-}PPh_2)$ (2.7540 (5) Å),[26] and in **3b** an appropriate comparison is with $Os_2(CO)_6(\mu\text{-}I)(\mu\text{-}PPh_2)$ (2.789 (1) Å).[27] All of these molecules are dibridged by a phosphido group and one other ligand.

In the iron complex **1b** the two Fe–P bond lengths are significantly different (Δ = 0.014 Å), indicating asymmetry in the phosphido bridge. In contrast the M(1)–P and M(2)–P distances in **2b** and **3b** are equivalent. A comparison of M–M and M–P bond lengths and M–P–M bond angles down the triad (Table VIII) reveals some interesting features. An increase of 0.16 Å in M(1)–M(2) distance and 0.125 Å (average) in M–P bond length from **1b** to **2b** is accompanied by a 0.3° change in M–P–M angle at the phosphido bridge. However, the same parameters change by 0.04 Å, 0.02 Å (average) and 0.6° from **2b** to **3b**. Clearly the increase in M–M bond length from **2b** to **3b** is not accompanied by a concomitant increase in the metal–phosphorus bond lengths from **2b** to **3b**, hence producing a larger M–P–M angle. One explanation of this effect is that the Os–P bonds in **3b** may be unusually strong in comparison.

The most remarkable changes in molecular parameters down the triad are concerned with the metal–acetylide interaction. Although the C(7)–C(8) distance does not change significantly from **1b** to **3b**, this is not unexpected since the short –C≡C– bond is relatively insensitive to minor electronic perturbations even at this level of accuracy. In fact the C(7)–C(8) bond length in **1b** (1.223 (4) Å) is only slightly longer than the comparable distance (1.21 Å) in acetylene.[2] However, there are significant changes in the orientation of the acetylide with respect to the two metals and the strengths of the metal–acetylide bonds down the group. The M(2) to C(7) (C_α) and M(2) to C(8) (C_β) distances (compare *d* and *e* in Table VIII) become quite distinctly more equivalent from **1b** to **3b**; the differences Δr are 0.203 Å (M = Fe), 0.132 Å (M = Ru), and 0.067 Å (M = Os). Thus down the triad the acetylide β-carbon atom tips toward M(2), and the C(7)–C(8) triple bond becomes more parallel to the M(1)–M(2) vector. Indeed the Os(2)–C(8) bond length in **3b** (2.377 (12) Å) is significantly *shorter* than the Ru(2)–C(8) bond (2.417 (3) Å) in **2b**. These structural changes are borne out by the magnitude of the angles C(7)–C(8)–C(9) (β) and M(1)–C(7)–C(8) (α). The former decreases from Fe to Ru to Os as the acetylide swings in toward the heavier metal and the latter decreases by fully 5.8° as the –C≡C– and M—M vectors approach parallelism. To our knowledge such changes are unprecedented and indicate significantly stronger metal–hydrocarbyl η interactions down the group. Such changes should manifest themselves in differences in reactivity profiles for the μ_2-η^2-hydrocarbyl group as the nature of the metal–ligand interaction is modified.

In recent years a number of other binuclear μ_2-η^2-alkynyl compounds have been structurally characterized including dirhenium,[21] dirhodium,[28] diplatinum,[29] and mixed-metal species.[30] A number of metal cluster compounds also contain μ_2-η^2 edge-bridging acetylides.[2] For most of these compounds the distortion of the acetylide from linearity is less than that in **3b**. Indeed in many cases the acetylide appears to be only lightly coordinated.[28,30a] The availability of structural and spectroscopic data for the entire series of molecules **1**–**3** described here should facilitate the further systematic development of useful chemistry already underway[2a,3a,3b,3f,21] for these compounds.

Acknowledgment. We are grateful to the Natural Sciences and Engineering Research Council of Canada for financial support of this work in the form of operating grants (to A.J.C.) and scholarships to (A.A.C. and L.H.R.).

Registry No. **1a**, 52970-25-9; **1b**, 59584-68-8; **1c**, 62475-91-6; **2a**, 82647-81-2; **2b**, 82647-83-4; **2c**, 112794-23-7; **3a**, 109976-28-5; **3b**, 112794-24-8; **3c**, 112794-25-9; $Fe_3(CO)_{12}$, 17685-52-8; $Fe_3(CO)_{11}(Ph_2PC{\equiv}CPh)$, 112794-26-0; $[Fe(CO)_4(Ph_2PC{\equiv}CPh)]$, 62415-28-5; $Ru_3(CO)_{12}$, 15243-33-1; $Ru_3(CO)_{11}(Ph_2PC{\equiv}CBu\text{-}t)$, 110511-62-1; $Os_3(CO)_{11}(Ph_2PC{\equiv}CPr\text{-}i)$, 82647-85-6; $Os_3(CO)_{12}$, 15696-40-9; $Os_3(CO)_9(\mu_3\text{-}\eta_2\text{-}C{\equiv}CPr\text{-}i)(\mu\text{-}PPh_2)$, 77681-76-6; $Os_3(CO)_{11}(Ph_2PC{\equiv}CPh)$, 112794-27-1; $Os_3(CO)_{11}(Ph_2PC{\equiv}CBu\text{-}t)$, 77674-39-6; $Os_3(CO)_{11}(MeCN)$, 65702-94-5; $Ph_2PC{\equiv}CPh$, 7608-17-5; $Ph_2PC{\equiv}CBu\text{-}t$, 33730-51-7; $Ph_2PC{\equiv}CPr\text{-}i$, 62199-59-1.

Supplementary Material Available: Table of ^1H NMR spectra (Table S1), anisotropic thermal parameters (Tables S2–S4), and phenyl ring distances and angles (Table S5) (7 pages); listings of structure factors (Tables S6–S8) (55 pages). Ordering information is given on any current masthead page.

(24) In $Fe_3(CO)_{12}$,[24a] $Ru_3(CO)_{12}$,[24b] and $Os_3(CO)_{12}$[24c] the unbridged M–M bond lengths average 2.673, 2.8542, and 2.877 Å, respectively. These values can be taken as representative of M–M single bond distances. (a) Wei, C. H.; Dahl, L. F. *J. Am. Chem. Soc.* **1969**, *91*, 1351. (b) Churchill, M. R.; Hollander, F. J.; Hutchinson, J. P. *Inorg. Chem.* **1977**, *16*, 2655. (c) Churchill, M. R.; DeBoer, B. G. *Inorg. Chem.* **1977**, *16*, 878.

(25) Taylor, N. J.; Mott, G. N.; Carty, A. J. *Inorg. Chem.* **1980**, *19*, 560.

(26) Mott, G. N.; Granby, R.; MacLaughlin, S. A.; Taylor, N. J.; Carty, A. J. *Organometallics* **1983**, *2*, 189.

(27) Geoffroy, G. L.; Rosenberg, S.; Herlinger, A. W.; Rheingold, A. L. *Inorg. Chem.* **1986**, *25*, 2916.

(28) Cowie, M. R.; Loeb, S. A. *Organometallics* **1985**, *4*, 852.

(29) Ciriano, M.; Howard, J. A. K.; Spencer, J. L.; Stone, F. G. A.; Wadepohl, H. *J. Chem. Soc., Dalton Trans.* **1979**, 1749.

(30) (a) Hutton, A. T.; Langrick, R. C.; McEwan, D. M.; Pringle, P. G.; Shaw, B. L. *J. Chem. Soc., Dalton Trans.* **1985**, 2121. (b) Salah, O. M. A.; Bruce, M. I.; Churchill, M. R.; DeBoer, B. G. *J. Chem. Soc., Chem. Commun.* **1974**, 688. (c) Yasufuku, K.; Yamazaki, H. *Bull Chem. Soc. Jpn.* **1972**, *45*, 2664.